ACS OMEGA

http://pubs.acs.org/journal/acsodf

Article

Identification of a New Chemotype of Anti-Obesity Compounds by Ensemble Screening

Hyunkyung Cho,[‖] Joo-Youn Lee,[‖] Sang Yoon Choi,[‖] Chaemin Lim, Min-Kyoung Park, Hyejin An, Jeong Ok Lee, Minsoo Noh, Seunghee Lee,* and Sanghee Kim*

Cite This: https://dx.doi.org/10.1021/acsomega.9b04454

Read Online

ACCESS | Metrics & More | Article Recommendations | Supporting Information

ABSTRACT: Despite the increasing prevalence of overweight or obesity in the global population, most of the approved drugs for obesity are still not ideal for long-term use due to severe cardiovascular and/or neurological side effects. Therefore, we designed a library-implemented virtual screening (VS) approach to discover new anti-obesity agents without significant toxicity. The Bayesian classification and 3D pharmacophore model for the VS process were built by using the screening results of our in-house library of natural piper amide-like compounds, which possess a wide range of biological activities and relatively low toxicities. The VS process identified six compounds of different classes with enhanced inhibitory activities against lipid accumulation and without toxicity. Moreover, the most active compound with an oxadiazole scaffold resulted in weight loss and improved the fatty liver condition of mice with overnutrition in animal experiments.

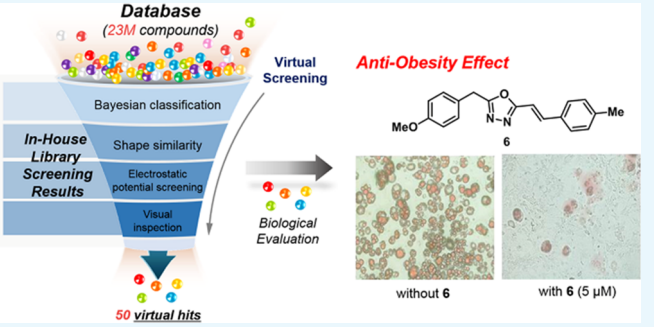

INTRODUCTION

Obesity is defined by the World Health Organization as abnormal or excessive fat accumulation in adipose tissue.[1] This abnormality is one of the most common global health problems for all age groups. The increase in the prevalence of obesity threatens individual health by exposure to the risk of associated complications, including type 2 diabetes, hyperlipidemia, hypertension, gallbladder disease, and certain types of cancers.[2] Accordingly, several pharmacotherapies have been developed for the prevention or treatment of obesity by targeting a variety of receptors and enzymes, such as intestinal lipase, 5-HT_{2C} receptor, β3 adrenergic receptor, GLP-1, and many other gut-derived peptides.[3] At present, five drugs are approved by the FDA for the treatment of obesity: orlistat, lorcaserin, phentermine/topiramate, bupropion/naltrexone, and liraglutide.[4] However, only orlistat and lorcaserin are approved for long-term use due to the severe adverse effects of the other drugs, such as cardiovascular and/or neurological side effects.[5,6] In this regard, the development of new anti-obesity agents without adverse side effects is still highly desirable.

Computer-based virtual screening (VS) has become a powerful technique for accelerating the drug discovery process and identifying new classes of drugs.[7,8] A large number of informatics tools and methods have been utilized for VS and can be classified broadly into two categories: ligand-based virtual screening (LBVS) and structure-based virtual screening (SBVS).[9] LBVS methods use ligand fragments and patterns from the known structure−activity data set to select candidates by similarity searching, pharmacophore mapping, quantitative structure−activity relationship (QSAR) modeling, or machine learning methods. On the other hand, SBVS involves protein−ligand docking with the 3D structural information of the biological target followed by ranking the ligands based on their corresponding docking score. Because of the great versatility of VS approaches, both LBVS and SBVS campaigns have been applied for the discovery of obesity-related bioactive molecules.[10] Several types of hit compounds against 13 obesity-relevant targets have been identified via LBVS or SBVS campaigns. Nevertheless, novel VS approaches are still necessary for seeking an unprecedented class of anti-obesity drugs and targets to cope with the complex molecular mechanisms related to the pathogenesis of obesity.[11]

Hence, in this manuscript, we present the library-implemented discovery of anti-obesity agents by a combined VS process. For the design of the VS filters, a natural piper amide-derived in-house library[12] and its screening results were utilized. Piper amide natural products might be a promising resource in the search for novel anti-obesity agents owing to their broad spectrum of biological features related to metabolic

Received: December 27, 2019
Accepted: February 6, 2020

homeostasis and relatively low toxicities.[13] For instance, piper amides from *Piper retrofractum* Vahl. have been reported to regulate lipid metabolism-related proteins and reduce weight gain in a high-fat diet (HFD)-induced mice model.[14] Thus, we envisioned that our in-house library compounds with natural piper amide scaffolds could be an excellent tool for discovering new anti-obesity agents because structurally similar compounds tend to have similar biological activity.[15] The presented VS approach implemented on a natural product-like library provided basis for finding next-generation weight reducing agents, and further in vitro and in vivo biological evaluation indicated that compound **6** (PubChem_CID, 6005418) has a great potential as a lead scaffold for a new class of anti-obesity agents.

RESULTS AND DISCUSSION

Screening a Piper Amide-like Compound Library for Anti-Obesity. Using the constructed natural piper amide-like compound library, which featured an α,β-unsaturated amide scaffold,[12] the lipid accumulation inhibitory effects of 228 compounds were tested on 3T3-L1 cells at 50 μM. 3T3-L1 preadipocytes have been extensively used in the study of adipocyte differentiation and lipid production. To rule out false positives and compounds with cellular toxicity, the cell viability rate was also examined by performing MTT assays. The resulting lipid reduction data (x axis) were plotted against cell viability (y axis) as a two-dimensional scatter plot (Figure 1).[16]

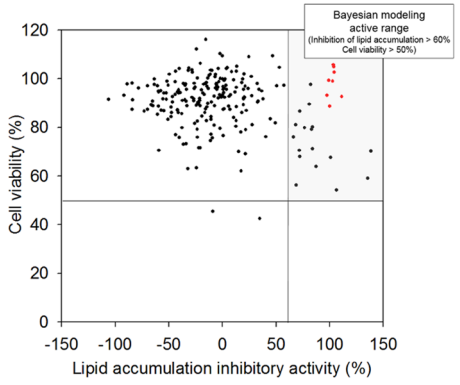

Figure 1. Library screening data and active compound range of Bayesian modeling. Cell viability and anti-adipogenic effects of 228 compounds were tested on 3T3-L1 cells at 50 μM. The 3T3-L1 cells were differentiated into adipocytes by day 8. Eight active compounds (NED-109, NED-223, NED-240, NED-241, NED-242, NED-262, NED-275, and NED-278) that were utilized in 3D pharmacophore modeling are shown as red dots.

The majority of the compounds exhibited relatively low toxicity even at a relatively high concentration of 50 μM, which might result from the natural product likeness of our library compounds.

Generation of the Bayesian Model. The Bayesian classification was primarily employed to identify the crucial structural elements of piper amides that contribute to anti-obesity activity.[17] Based on the library screening results shown in Figure 1, compounds exhibiting greater than 60% inhibitory activity against lipid accumulation with cell viability >50% were designated as "active", and the rest were designated as "inactive". All 228 data set molecules were divided randomly into the training set (181 compounds) and test set (47 compounds) by using the random percent filter (training:test = 80:20). Additionally, the following nine descriptors were calculated by Pipeline Pilot 2016[18] and selected to construct a reliable model: AlogP, molecular weight, number of rotatable bonds, number of rings, number of aromatic rings, number of hydrogen bond donors, number of hydrogen bond acceptors, molecular fractional polar surface area, and ECFP_6 (extended-connectivity fingerprints at maximum diameter 6).[19] The constructed model was validated by a leave-one-out cross-validation process, and the area under the receiver operating characteristic (ROC) curve for the score in the training set was found to be 0.838, indicating the "good" accuracy of the model (the ROC plots are shown in Figure S1).[20] For the test set validation, the best split was calculated by selecting the split that minimized the sum of the percentage misclassified category members and nonmembers using the cross-validated score for each compound. A contingency table (Table 1) was generated containing the numbers of true positives (TP), false negatives (FN), false positives (FP), and true negatives (TN).

Table 1. Results of the Naïve Bayesian Model[a]

	active		inactive					
set	TP	FN	FP	TN	ROC	SE	SP	Q
training	21	1	25	134	0.838	0.955	0.843	0.856
test	3	0	9	35	0.992	1.000	0.795	0.809

[a]TP, true positive; FN, false negative; FP, false positive; TN, true negative; ROC, the area under the receiver operating characteristic curve score; SE, sensitivity, SE = TP/(TP + FN); SP, specificity, SP = TN/(TN + FP); Q, overall accuracy, Q = (TP + TN)/(TP + TN + FP + FN).

A test set consisting of 47 compounds was applied to validate the Bayesian classification model. The ROC score in the test set was 0.992, which indicates that our model is excellent at distinguishing between the active and inactive. Furthermore, the calculated sensitivity, specificity, and accuracy for the test set were increased compared to those of the training set (Table 1). These outcomes demonstrated that the established classification model has good performance in identifying the vital fragment present in library compounds with the anti-obesity effects.

Generation of the Field-Based Common Pharmacophore Model. To improve the accuracy of VS, we generated a field-based common pharmacophore model, which included 3D structural features of ligands. In this study, we chose the eight active compounds NED-109, NED-223, NED-240, NED-241, NED-242, NED-262, NED-275, and NED-278 (Figure 2) from the results of inhibitory activity in lipid accumulation (%) with cell viability (%) values among all 228 compounds. The 3D conformations of each eight active compound were generated using FieldTemplater (Forge v.10.3),[21] and the conformers of each compounds were populated using Xedex,[22] a component of Forge. Each conformation was exhaustively compared pairwise until the field point pattern became common for active compounds as many as possible. After scoring the 760 generated template models, we selected the best model by consensus alignment based on the three-dimensional field point patterns. The selected best model mapped six compounds (NED-240, NED-241, NED-242, NED-262, NED-275, and NED-278) out of eight active compounds, and the field and shape similarity scores were 0.746 and 0.832, respectively. Through analyzing the common

https://dx.doi.org/10.1021/acsomega.9b04454
ACS Omega XXXX, XXX, XXX−XXX

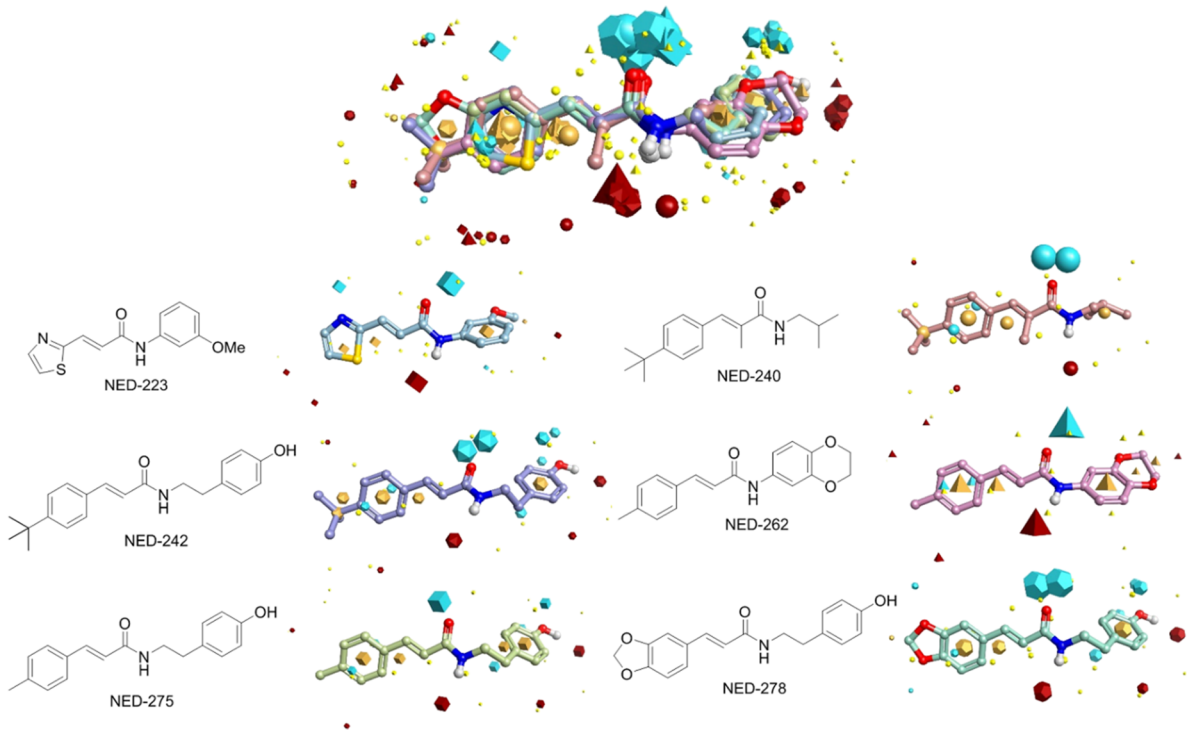

Figure 2. Identification of the common pharmacophore of six active compounds (NED-223, NED-240, NED-242, NED-262, NED-275, and NED-278) on the basis of field points. Field-based template models containing a single conformation of compounds NED-223 (sky blue), NED-240 (pale pink), NED-242 (purple), NED-262 (pink), NED-275 (lime green), and NED-278 (teal green). Negatively charged field points are shown in blue; positively charged field points are red; van der Waals/shape field points are displayed in yellow; centers of hydrophobicity are shown in orange. Larger field points represent stronger points of potential interaction.

field point patterns, we recognize that the positive and negative electrostatic fields near the amide bond are mostly consistent because all active compounds share the amide scaffold. Additionally, hydrophobic fields are prevalent along the α,β-unsaturated aromatic or heteroaromatic rings of the active compounds. This indicates that hydrophobic aromatic groups adjacent to the double bonds are favorable for anti-adipogenic activity. The additional negative field points surrounding the phenolic moieties of NED-242, NED-275, and NED-278 are observed only in those three molecules but possibly correlate with the inhibitory activity. With this in mind, we performed VS to seek new classes of active compounds.

Library-Focused Virtual Screening Combined Bayesian and Field-Based Model. To discover new scaffolds for anti-obesity compounds, we conducted VS based on the generated Bayesian model and 3D field point patterns. We combined the machine learning model and 3D similarity search to obtain improved performance by analyzing both 2D and 3D structural properties of compounds. The steps combined 2D fingerprint classification using naïve Bayesian and 3D VS using ROCS and EON procedures, as shown schematically in Figure 3.

As the first step of VS, the chemical library of Korea Chemical Bank was screened virtually using the Bayesian model. Among the 222,960 molecules, 90,459 compounds were predicted by our 2D classification model to have anti-obesity effects. Then, the selected compounds were prepared for the 3D similarity search by performing conformational energy minimization with Omega v.2.5 in the OpenEye package.[23,24] Up to 200 conformers for each molecule were generated for the first 90,459 compounds screened. For these conformers, shape-based similarity searching and electrostatic

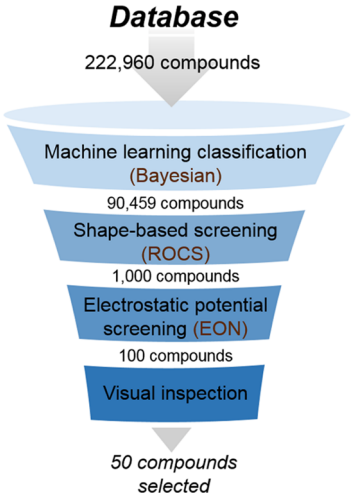

Figure 3. Schematic of virtual screening.

potential matching steps were conducted in a process using ROCS and EON tools based on the obtained conformations of the six active compounds derived from the field-based pharmacophore model. As a result of the workflow, the top 100 candidates were chosen from the large compound database. Additional visual inspection was carried out to exclude false-positive compounds. Accordingly, 50 candidates were finally selected for examining anti-adipogenic activity in vitro.

In Vitro Screening for Anti-Obesity Effects of the Selected Compounds. The 50 virtual hits were experimentally evaluated for anti-obesity effects. To unambiguously

https://dx.doi.org/10.1021/acsomega.9b04454
ACS Omega XXXX, XXX, XXX−XXX

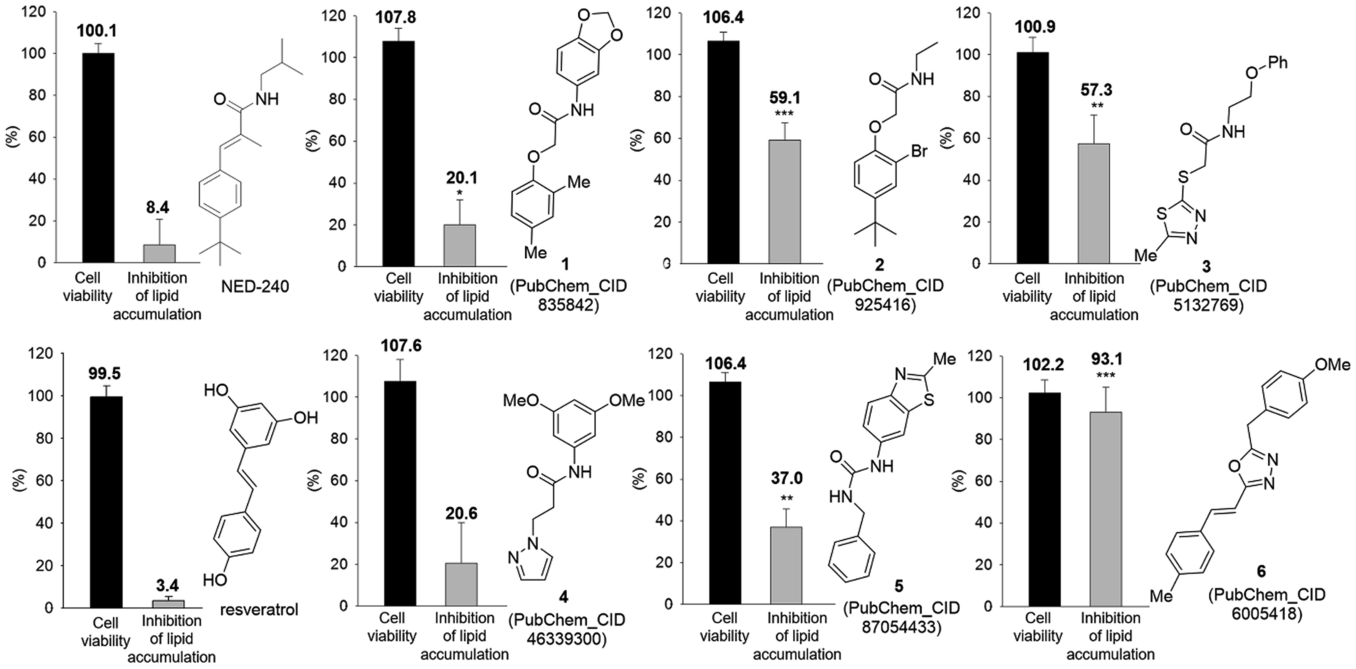

Figure 4. Assay results and chemical structures of six active compounds **1**−**6**, NED-240, and resveratrol. Cell viability and anti-adipogenic effects of compounds were assayed on 3T3-L1 cells at 5 μM. Three independent experiments were conducted. *p < 0.05, **p < 0.01, ***p < 0.005, significantly different from the induction group.

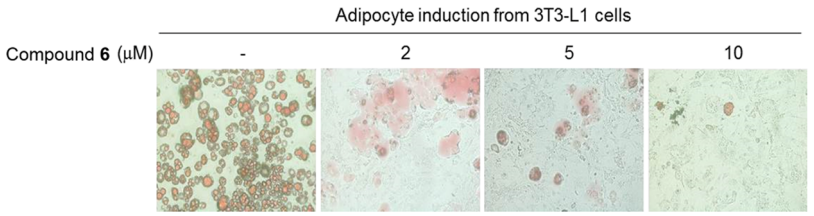

Figure 5. Effect of compound **6** on adipocyte differentiation from 3T3-L1 cells. Oil red O staining shows significant inhibition of lipid accumulation by compound **6**.

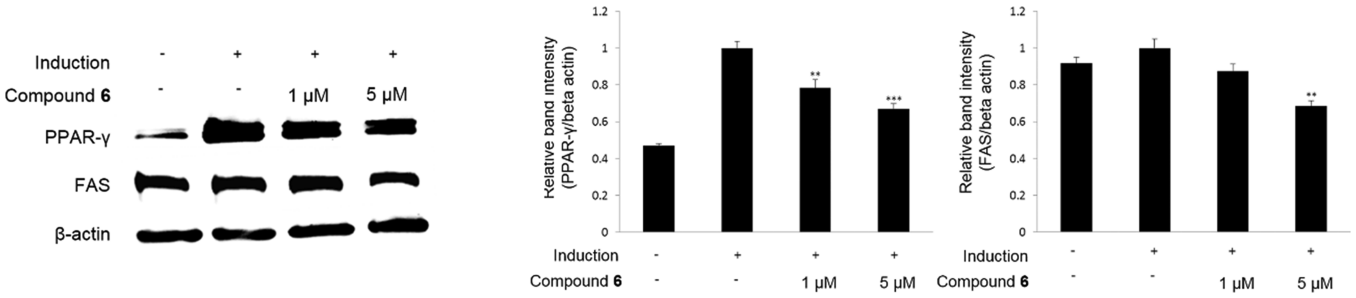

Figure 6. Effect of compound **6** on the expression of PPAR-γ and FAS in adipocytes from 3T3-L1 cells. Protein expression was evaluated via western blot analysis. *p < 0.05, **p < 0.01, ***p < 0.005, significantly different from the induction group.

identify the compounds that exhibited inhibitory activity against lipid accumulation, we examined the effects of compounds on adipogenesis using 3T3-L1 cells at 5 μM. As positive controls, resveratrol and one of the most active natural piper amide derivatives, NED-240, were used. Six compounds were found to inhibit hormone-induced adipocyte differentiation and lipid accumulation with similar or higher activity than positive controls (Figure 4). A notable feature is that the obtained six compounds exhibited no significant cellular toxicity. Five selected compounds contain an amide group. Two of them, **1** and **2**, have an α-phenoxyacetamide moiety, and one compound **3** has an α-thioacetamide. Amide compound **4** contains a pyrazole ring at the β-position. Compound **5** is the urea derivative with a benzothiazole ring. Unlike these compounds, compound **6** does not contain an amide moiety but does have an oxadiazole moiety.

The positive control, NED-240, showed only weak inhibition of lipid accumulation at a tested concentration of 5 μM. Compared to NED-240, the structurally similar compound **2**, in which the *p*-(*tert*-butyl)pheny group is still present, considerably suppressed lipid accumulation. Compound **3** with the α-thioacetamide group also suppressed lipid accumulation to a similar extent to **2**. Interestingly, oxadiazole **6** showed the most significant inhibition of lipid accumulation.

https://dx.doi.org/10.1021/acsomega.9b04454
ACS Omega XXXX, XXX, XXX−XXX

The IC_{50} of **6** was 0.6 μM, which is much lower than that of resveratrol (29.8 μM). Accordingly, further biological evaluation of **6** was performed.

Biological Effect of 6 on Adipogenesis and Lipid Accumulation in 3T3-L1 Adipocytes. The inhibitory activity of **6** in adipocyte induction from 3T3-L1 cells was also confirmed in a dose-dependent manner by oil red O staining, as shown in Figure 5. To understand the molecular mechanism underlying the anti-adipogenic effect of **6**, the expression levels of key transcription factors involved in adipocyte differentiation and adipogenic genes involved in lipogenesis and metabolism were analyzed. The expression of peroxisome proliferator-activated receptor (PPAR)-γ, which is well known to regulate adipogenesis, lipid metabolism, and obesity,[25] was significantly inhibited by compound **6** in 3T3-L1 cells in a dose-dependent manner (Figure 6).[26]

Fatty acid synthase (FAS) is another central enzyme in lipogenesis, and thus, the increased expression and/or activity of FAS is related to the development of various diseases, including obesity.[27] Indeed, our western blot analysis also showed that **6** reduced the expression of FAS in a dose-dependent manner. These results suggest that oxadiazole **6** exerts an anti-adipogenic effect by inhibiting the expression of master adipogenic transcription factor and its target genes. The differentiation of preadipocytes is regulated by a complex network of multiple transcription factors to modulate the expression of genes that are responsible for adipocyte development; thus, further investigation is needed to define how the expression of PPAR-γ is regulated by compound **6**, for example, whether it suppresses the upstream transcription factors directly or not.

In Vivo Investigation of the Anti-Obesity Activity of Compound 6. To test the anti-obesity effect of compound **6**, C57BL/6 N mice were fed a normal chow diet (CD) or HFD for 12 weeks and then treated with vehicle, compound **6**, and resveratrol per os (PO) for 8 days. The anti-obesity effect of resveratrol is one of its very well-known physiological activities, which also include anti-oxidative, anticancer, and cardiovascular protective functions, and resveratrol is thus used as a positive control.[28] There was no difference in food intake between the HFD group and the HFD plus compound **6** or resveratrol groups (data not shown). However, compound **6**-treated mice showed a significantly decreased body weight that was similar to that of resveratrol-treated mice compared with the HFD group (Figure 7).

Next, to evaluate the effect of compound **6** on fatty liver formation by HFD, we examined the liver tissue of each group. The gross morphology of the livers was enlarged, and a yellowish color was observed in the livers of mice fed with a HFD, indicating accumulation of lipids compared with that in the livers of CD control mice. However, this morphological change was reversed by treatment with compound **6** or resveratrol (Figure 8a). Consistently, the liver weight per body weight was increased in mice with HFD but was significantly reduced to the normal level by treatment with compound **6** or resveratrol (Figure 8b).

Histological analyses of the liver tissues by hematoxylin and eosin (H&E) staining revealed high accumulation of a microvesicular-type fat in the cytoplasm of the hepatocytes in HFD-fed mice compared with the lean control mice, which was further confirmed by oil red O staining (Figure 9). Lean mice fed with the normal chow diet showed little histological evidence of fat deposition. Furthermore, the administration of compound **6** or resveratrol for 8 days significantly reduced the accumulation of fat in hepatocytes compared with that in mice fed with the HFD alone.

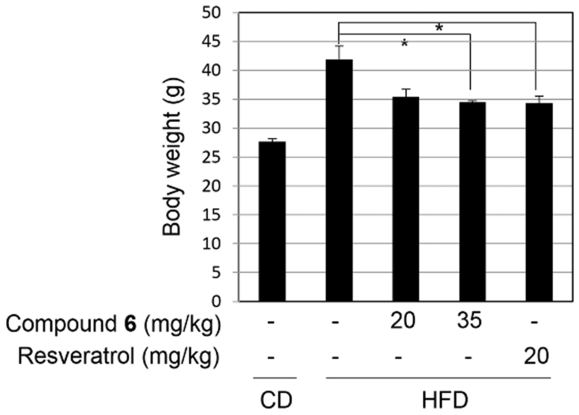

Figure 7. Effect of compound **6** on body weight gain in C57BL/6 N mice fed a HFD. Compound **6** or resveratrol was administered orally at doses of 20 and 35 mg/kg every day for 8 days. The HFD and CD control groups were administered a vehicle. Data are presented as the mean ± SEM (n = 5–7). *p < 0.05, significantly different from the HFD group.

Our results clearly showed that compound **6** exhibited anti-obesity activity in HFD mice, which is consistent with the anti-adipogenic effect on 3T3-L1 adipocyte differentiation.

CONCLUSIONS

In this manuscript, we present an efficient VS protocol implemented on a natural product-like library that combined 2D and 3D approaches to discover new chemotypes of anti-obesity agents. We developed multistage VS on the basis of the biological screening results of our in-house natural piper amide-like library, which enables the time-efficient prediction of anti-obesity activity. A total of 222,960 commercially available compounds were applied to the VS procedure, and 50 compounds were selected for the biological assay. Among the selected compounds, several different types of compounds were identified as hit compounds. They showed similar or higher inhibitory effects on lipid accumulation in 3T3-L1 cells without significant toxicity than the initial hit natural piper amide-like molecule, NED-240. The hit rate of the performed VS was calculated to be 12.0%, which suggested that the integrated natural product-like library-focused VS protocol was quite reliable for identifying new promising chemical candidates possessing anti-obesity activity. Moreover, the most potent compound **6** with a unique oxadiazole scaffold was validated as a potential anti-obesity agent through in vitro and in vivo biological investigations. Treatment with compound **6** led to a significant reduction in body and liver weight and suppressed fatty liver formation, possibly through modulating the expression or activity of adipogenic transcription factors and their downstream target genes involved in adipocyte development and lipogenesis. We believe that compound **6** discovered in this work can serve as a lead for anti-obesity drug discovery, although its mechanism of action (MOA) has not yet been clearly elucidated. Lead optimization and further pharmacological and pharmacokinetic study of compound **6** are in progress, and these results will be reported in due course.

https://dx.doi.org/10.1021/acsomega.9b04454
ACS Omega XXXX, XXX, XXX−XXX

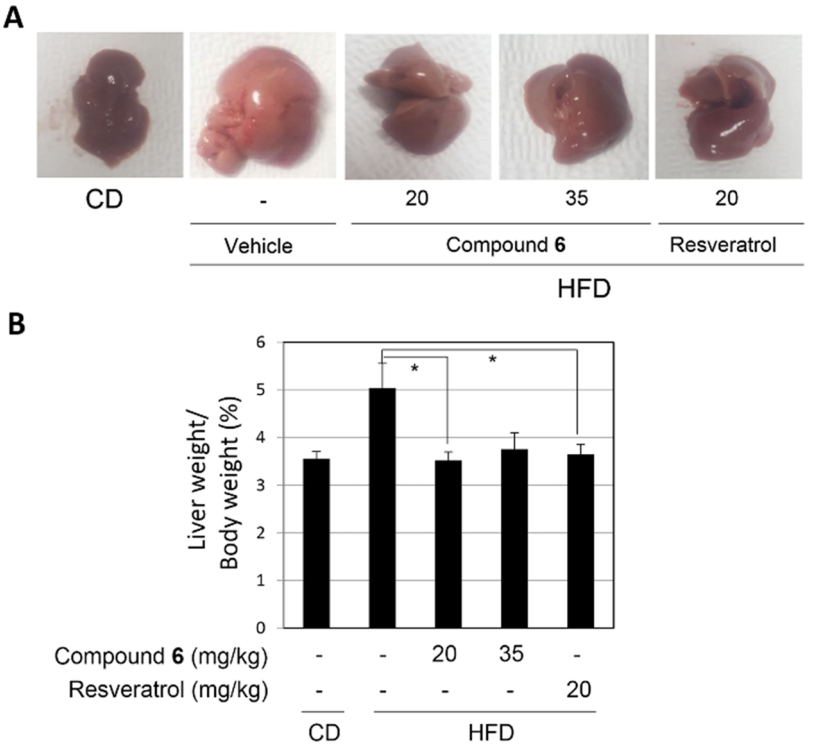

Figure 8. Inhibition of HFD-induced steatosis by compound **6**. (A) Gross morphology of livers from each group fed normal CD or HFD for 12 weeks plus vehicle, compound **6**, and resveratrol. (B) Liver weight per body weight was measured. Compound **6** or resveratrol-treated groups were administered orally at doses of 20 and 35 mg/kg every day for 8 days. The HFD and CD control groups were administered a vehicle. Data are presented as the mean ± SEM (n = 5−7). *p < 0.05, significantly different from the HFD group.

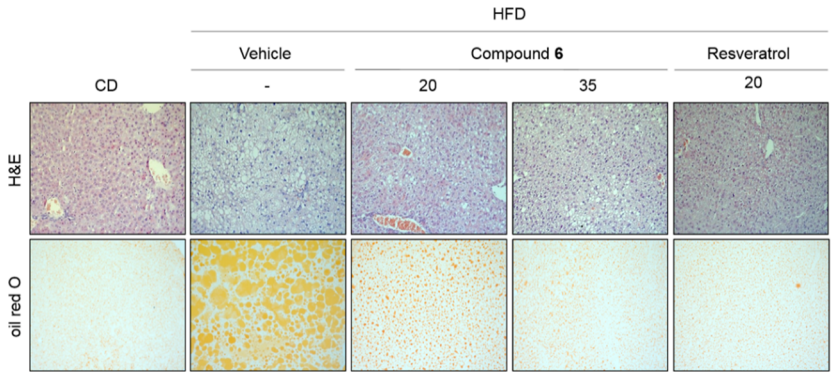

Figure 9. Effects of compound **6** treatment on hepatic steatosis in HFD mice. H&E and oil red O staining of the liver showed significant improvement of fatty liver formation by compound **6** and resveratrol.

METHODS

Chemistry. A set of 228 natural product-like library compounds was prepared from our previous study,[12] and 50 selected compounds from VS were provided by Korea Chemical Bank. The purity of the compounds was stated by providers to be ≥95%. The purity of the active compounds was also confirmed by our laboratory Additionally, the most potent compound **6** was synthesized on a large scale in our laboratory for further biological evaluations according to the following procedure (Scheme 1). All chemicals were of reagent grade and used as received. All reactions were performed under an inert atmosphere under dry nitrogen using distilled dry solvents. Reactions were monitored by TLC analysis using silica gel 60 F-254 thin-layer chromatography plates. Flash column chromatography was performed on silica gel (230−400 mesh). Melting points were measured using a Buchi B-540 melting point apparatus without correction. ^{1}H NMR (300 or 500 MHz) and ^{13}C NMR (125 MHz) spectra were recorded in δ units relative to the nondeuterated solvent as the internal reference. IR spectra were measured on a Fourier transform

Scheme 1. Synthetic Route of Compound 6[a]

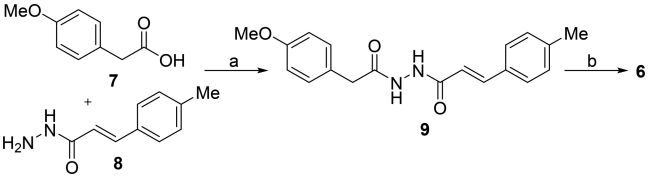

[a]Reagents and conditions: (a) EDCI, DMF, rt, 19 h, 88%; (b) $POCl_3$, 80 °C, 21 h, 93%

https://dx.doi.org/10.1021/acsomega.9b04454
ACS Omega XXXX, XXX, XXX−XXX

infrared spectrometer. High-resolution mass spectra (HRMS) were recorded using fast atom bombardment (FAB).

Synthetic Procedure of Compound ***6****. (E)-N′-(2-(4-Methoxyphenyl)acetyl)-3-(p-tolyl)acrylohydrazide (9).*[29] Compound **9** was synthesized from hydrazide compound **8**, which was prepared according to the published procedure.[30] To a solution of compound **8** (4.0 g, 22.9 mmol) in DMF (230 mL), 4-methoxyphenylacetic acid **7** (3.8 g, 22.9 mmol) and *N*-(3-dimethylaminopropyl)-*N*′-ethylcarbodiimide hydrochloride (5.3 g, 27.4 mmol) were added. Then, the mixture was stirred at rt for 19 h and concentrated in vacuo. The obtained crude mixture was filtered with CH2Cl2 (50 mL) three times to afford the desired hydrazide analog **9** (6.5 g, 20.1 mmol, 88%) as a white solid; 1H NMR (300 MHz, DMSO-d_6) δ 10.42 (br s, 1H), 10.28 (br s, 1H), 7.01 (t, J = 6.8 Hz, 3H), 7.40 (d, J = 8.7 Hz, 4H), 7.04 (d, J = 9.0 Hz, 2H), 6.77 (d, J = 15.9 Hz, 1H), 3.92 (s, 3H), 3.60 (s, 2H), 2.49 (s, 3H).

(E)-2-(4-Methoxybenzyl)-5-(4-methylstyryl)-1,3,4-oxadiazole (6).[29] Hydrazide **9** (4.0 g, 12.3 mmol) was suspended in $POCl_3$ (62 mL). The reaction was heated at 80 °C and stirred for 21 h. Afterward, the mixture was quenched by the addition of 2 N solution of NaOH at 0 °C. The residue was extracted three times with EtOAc. The combined organic layer was washed with brine, dried over $MgSO_4$, and concentrated in vacuo. The residue was purified by flash chromatography on silica gel (R_f = 0.30, hexane/EtOAc, 4:1) to obtain the oxadiazole **6** as a white solid (3.5 g, 11.4 mmol, 93%); m.p. 105−107 °C; ^{1}H NMR (CD_2Cl_2, 500 MHz) δ 7.43 (t, J = 7.1 Hz, 3H), 7.26 (d, J = 8.5 Hz, 2H), 7.20 (d, J = 8.0 Hz, 2H), 6.93 (d, J = 16.5 Hz, 1H), 6.88 (d, J = 8.7 Hz, 2H), 4.14 (s, 2H), 3.77 (s, 3H), 2.35 (s, 3H); ^{13}C NMR (CD_2Cl_2, 125 MHz) δ 165.4, 165.2, 159.4, 140.7, 138.7, 132.4, 130.3 (2C), 130.0 (2C), 127.7 (2C), 126.5, 114.5 (2C), 109.4, 55.6, 31.3, 21.5; IR (CH_2Cl_2) υ_{max} = 2931, 1611, 1534, 1514, 1250, 1179, 1033, 969, 806 cm^{-1}; high-resolution mass spectrometry (HRMS; FAB) calcd. $C_{19}H_{19}N_2O_2$ 307.1447 ($[M + H]^+$), found 307.1450.

Computational Details. *Data Sets.* A set of 228 compounds and their biological activities expressed in inhibition of lipid accumulation (%) and CV (%) rate were selected as a data set to perform classification using 2D descriptors. Among them, the top six bioactive compounds were taken as a template for 3D shape-based VS. The chemical library database for VS collected commercially available compounds from Korea Chemical Bank. The 222,960 compounds were obtained from diverse suppliers, such as Asinex, ChemBridge, ChemDiv, Enamine, and TimTec. All 2D structures were prepared using Pipeline Pilot 2016.[18]

Bayesian Classification. A Bayesian model is an effective machine learning method to classify active and inactive compounds using 2D descriptors. A total of 228 biaryl amide analogs experimentally known for their anti-obesity effects were collected in our previous study. If a compound had lipid accumulation inhibitory effects greater than 60% with a CV rate of greater than 50%, then it was defined as active; other compounds were defined as inactive. The descriptors used include AlogP, molecular weight, number of aromatic rings, number of hydrogen bond acceptors, number of hydrogen bond donors, number of rings, number of rotatable bonds, molecular fractional polar surface area, and extended-connectivity fingerprints (ECFP_6). All data were split randomly into the training and validation sets using the "Generate Training and Test Data" protocol implemented in Pipeline Pilot 2016.[18] Then, the "Create Bayesian Model" protocol in Pipeline Pilot was employed to perform the Laplacian-modified Bayesian analysis to build a model, and a leave-one-out cross-validation ROC curve was obtained. The good and bad features of training set compounds present in the biaryl amide analogs play a crucial role in the anti-obesity effect.

Field-Based Pharmacophore Alignment. The most active compounds, NED-109, NED-223, NED-240, NED-241, NED-242, NED-262, NED-275, and NED-278 were selected to create a potential bioactive conformation model using the shape and field point from the ligands. The conformations of each eight compounds were collected to a maximum of 200 structures using Cresset's Xedex embedded with Forge. The 3D field point pattern for each conformations of each eight compounds was calculated and used to cross-compare to each other using FieldTemplater (conducted within Forge v.10.3)[21] as fraction of score from a shape similarity set of 0.5, that is, default setting. The minimum molecules per template set are 5 in this case. The top 3D field alignment model was selected where the resulting templates included six compounds among eight compounds. The highly active six compounds in order by lipid inhibition (%) with CV (%) value were included in the selection model. The proposed templates each consist of one conformation of six active compounds, which are NED-223, NED-240, NED-242, NED-262, NED-275 and NED-278.

Shape- and Electrostatic-Based 3D Virtual Screening. Rapid overlay of chemical structures (ROCS) can rapidly calculate potentially active compounds by shape comparison. The generation of the low-energy conformers of the 90,459 library compounds, which was preselected using Bayesian modeling, was performed with OMEGA v.2.5[24] using default settings, thereby generating a maximum number of 200 conformers for each molecule. The field- and shape-based aligned conformer of six bioactive compounds that result from the FieldTemplater calculation were used as query for the 3D virtual screening using ROCS v.3.2.[31] The best 1000 hits were screened, considering the ROCS_TanimotoCombo score. Then, we performed an electrostatic comparison for the screened 1000 compounds using EON v.2.2,[32] and the only top 100 hits were selected by the EON_ET_combo score for each six query. Duplicate compounds among the results from each query were removed, and 50 compounds were finally selected for in vitro testing.

Biological Details. *Cell Culture.* 3T3-L1 cells were incubated using a DMEM media containing 10% FBS at 37 °C, 5% CO_2. 3T3-L1 cells were fully grown in a 48-well plate and treated with a hormone mixture (10 μg/mL insulin, 0.5 μM dexamethasone, 0.5 mM IBMX) for 48 h, and then, the media was changed to DMEM media containing insulin. Then, the cells were treated with test samples for 8 days, and the differentiation to adipocytes was observed.

Cell Viability Measurement. After the completion of cell differentiation, 0.5 mg/mL MTT [3-(4,5-dimethylthiazol-2-yl)-2,5-diphenyltetrazolium bromide] was added and incubated at 37 °C for 4 h. The MTT solution was eliminated; then, 200 μL of DMSO was added, and the absorbance was measured at 540 nm for cell viability.

Oil Red O Staining and Quantification. Upon completion of cell differentiation, the cells were rinsed with PBS twice and then fixed with 3.7% formaldehyde. The cells were incubated with oil red O dye for 1 h, and microscope images were taken to visualize red lipid droplets staining in differentiated cells.

https://dx.doi.org/10.1021/acsomega.9b04454
ACS Omega XXXX, XXX, XXX−XXX

Isopropanol was added, and the absorbance was measured at 510 nm for quantification.

Western Blot Analysis. After lysis, the 3T3-L1 cells were centrifuged at 14,000 rpm for 5 min, the supernatant was collected, and the protein was quantified using the Bradford (Bio-Rad, USA) reagent. Electrophoresis for 30 μg of protein was performed using SDS-PAGE and then transferred to a nitrocellulose membrane, and then, blotting was performed using FAS and the PPAR-γ antibody. Then, they were reacted with the HRP-conjugated secondary antibody and detected using ECL.

Animals and Experimental Design. All mouse work was performed under an approved protocol by the Institutional Animal Care and Use Committee of Seoul National University. Five-week-old C57BL/6 N mice, with a body weight of around 20 g, were purchased from Central Lab Animals Inc. and acclimated for 1 week. All mice were randomly divided into five groups (n = 7 per group): normal chow diet (10 kcal% fat) control group, high-fat diet (60 kcal% fat) control group, and high-fat diet with compound **6** or resveratrol groups. The compound **6**-treated group was treated with compound **6** at a dose of 20 and 35 mg/kg, and the normal and high-fat diet control groups were given distilled water. Compound **6** or water was orally administered to the mice for 8 days by gavage every day. Body weight and daily food intake were measured every day during the treatment.

Liver Weights and Histological Examination. The liver tissues from each mouse were removed and weighed. For histological analyses, liver tissues were fixed in 10% formalin solution and embedded in paraffin. Sections of 10 mm thickness were cut, stained with hematoxylin and eosin, viewed under an optical microscope, and photographed. For oil red O staining, mouse livers were frozen in an optimal cutting temperature compound, mounted on slides, and dried for 1−2 h at rt before sectioning. The sections were fixed with 4% paraformaldehyde for 10 min and stained in 0.5% oil red O solution in propylene glycol for 30 min. The slides were rinsed in distilled water and processed for hematoxylin counter staining.

■ ASSOCIATED CONTENT

Supporting Information

The Supporting Information is available free of charge at https://pubs.acs.org/doi/10.1021/acsomega.9b04454.

Library compounds distribution per lipid reduction activity, the ROC and enrichment plots of the Bayesian classification model, immunofluorescence analysis result of **6**, computational and biological data of the 50 virtual hits, purity analysis of hit compounds, and ^{1}H and ^{13}C NMR copies of **6** (PDF)

■ AUTHOR INFORMATION

Corresponding Authors

Seunghee Lee − *College of Pharmacy, Seoul National University, Seoul 08826, Korea*; Email: leeseung@snu.ac.kr

Sanghee Kim − *College of Pharmacy, Seoul National University, Seoul 08826, Korea*; orcid.org/0000-0001-9125-9541; Email: pennkim@snu.ac.kr

Authors

Hyunkyung Cho − *College of Pharmacy, Seoul National University, Seoul 08826, Korea*

Joo-Youn Lee − *College of Pharmacy, Seoul National University, Seoul 08826, Korea; Chemical Data-Driven Research Center, Korea Research Institute of Chemical Technology, Daejeon 34114, Korea*

Sang Yoon Choi − *Korea Food Research Institute, Wanju-gun, Jeollabuk-do 55365, Korea*

Chaemin Lim − *College of Pharmacy, Seoul National University, Seoul 08826, Korea*

Min-Kyoung Park − *College of Pharmacy, Seoul National University, Seoul 08826, Korea*

Hyejin An − *College of Pharmacy, Seoul National University, Seoul 08826, Korea*

Jeong Ok Lee − *College of Pharmacy, Seoul National University, Seoul 08826, Korea*

Minsoo Noh − *College of Pharmacy, Seoul National University, Seoul 08826, Korea*; orcid.org/0000-0002-4020-5372

Complete contact information is available at: https://pubs.acs.org/10.1021/acsomega.9b04454

Author Contributions

[‖]H.C., J.-Y.L., and S.Y.C. contributed equally to this work. All authors have given approval to the final version of the manuscript.

Notes

The authors declare no competing financial interest.

[#]C.L. is a chief scientific officer of A2A Pharmaceuticals in New York.

■ ACKNOWLEDGMENTS

This research was supported by a grant of the Korea Health Technology R&D Project through the Korea Health Industry Development Institute (KHIDI), funded by the Ministry of Health & Welfare, Republic of Korea (HI17C0447), and the Medical Research Center (MRC) (NRF-2018R1A5A2024425) through the National Research Foundation of Korea (NRF) funded by the Ministry of Science, ICT, and future Planning (MSIP). This research was also supported by Basic Science Research Program through the National Research Foundation of Korea (NRF) funded by the Ministry of Education (NRF-2019R1A6A3A01096019) and the Korea Food Research Institute (E0186701-02). Additionally, the chemical library for VS process was kindly provided by Korea Chemical Bank (www.chembank.org) of Korea Research Institute of Chemical Technology.

■ ABBREVIATIONS

VS, virtual screening; 5-HT, 5-hydroxytryptamine; GLP-1, glucagon-like peptide-1; FDA, Food and Drug Administration; LBVS, ligand-based virtual screening; SBVS, structure-based virtual screening; QSAR, quantitative structure−activity relationship; CV, cell viability; ECFP_6, extended-connectivity fingerprints at maximum diameter 6; ROC, receiver operating characteristic; PPAR-γ, peroxisome proliferator-activated receptor gamma; FAS, fatty acid synthase; CD, chow diet; HFD, high-fat diet

■ REFERENCES

(1) World Health Organization. *Obesity and overweight fact sheet*; https://www.who.int/en/news-room/fact-sheets/detail/obesity-and-overweight (accessed Feb 16, 2018).

(2) Haslam, D. W.; James, W. P. T. Obesity. *The Lancet* **2005**, *366*, 1197−1209.

(3) Bhat, S. P.; Sharma, A. Current drug targets in obesity pharmacotherapy − a review. *Curr. Drug Targets* **2017**, *18*, 983−993.
(4) Bonamichi, B. D. S. F.; Parente, E. B.; dos Santos, R. B.; Beltzhoover, R.; Lee, J.; Salles, J. E. N. The challenge of obesity treatment: a review of approved drugs and new therapeutic targets. *J. Obes. Eat. Disord.* **2018**, *04*, 1−10.
(5) Jones, B. J.; Bloom, S. R. The new era of drug therapy for obesity: the evidence and the expectations. *Drugs* **2015**, *75*, 935−945.
(6) Halpern, B.; Halpern, A. Safety assessment of FDA-approved (orlistat and lorcaserin) anti-obesity medications. *Expert Opin. Drug Saf.* **2015**, *14*, 305−315.
(7) Lavecchia, A.; Di Giovanni, C. Virtual screening strategies in drug discovery: a critical review. *Curr. Med. Chem.* **2013**, *20*, 2839−2860.
(8) Slater, O.; Kontoyianni, M. The compromise of virtual screening and its impact on drug discovery. *Expert Opin. Drug Discovery* **2019**, *14*, 619−637.
(9) Leach, A. R.; Gillet, V. J. Virtual screening. In *An Introduction to Chemoinformatics*, Revised ed.; Springer: Dordrecht, Netherlands, 2007; pp 159−181.
(10) Markt, P.; Herdlinger, S.; Schuster, D. Virtual screening against obesity. *Curr. Med. Chem.* **2011**, *18*, 2158−2173.
(11) Oh, S.; Kim, K. S.; Chung, Y. S.; Shong, M.; Park, S. B. Anti-obesity agents: a focused review on the structural classification of therapeutic entities. *Curr. Top. Med. Chem.* **2009**, *9*, 466−481.
(12) Kim, S.; Lim, C.; Lee, S.; Lee, S.; Cho, H.; Lee, J.-Y.; Shim, D. S.; Park, H. D.; Kim, S. Column chromatography-free solution-phase synthesis of a natural piper-amide-like compound library. *ACS Comb. Sci.* **2013**, *15*, 208−215.
(13) Gutierrez, R. M.; Gonzalez, A. M.; Hoyo-Vadillo, C. Alkaloids from piper: a review of its phytochemistry and pharmacology. *Mini Rev. Med. Chem.* **2013**, *13*, 163−193.
(14) Kim, K. J.; Lee, M.-S.; Jo, K.; Hwang, J.-K. Piperidine alkaloids from *Piper retrofractum* Vahl. protect against high-fat diet-induced obesity by regulating lipid metabolism and activating AMP-activated protein kinase. *Biochem. Biophys. Res. Commun.* **2011**, *411*, 219−225.
(15) Chen, B.; Greenside, P.; Paik, H.; Sirota, M.; Hadley, D.; Butte, A. J. Relating chemical structure to cellular response: an integrative analysis of gene expression, bioactivity, and structural data across 11,000 compounds. *CPT Pharmacometrics Syst. Pharmacol.* **2015**, *4*, 576−584.
(16) The detailed library compounds distribution per lipid reduction activity is described in Table S1.
(17) Xia, X.; Maliski, E. G.; Gallant, P.; Rogers, D. Classification of kinase inhibitors using a Bayesian model. *J. Med. Chem.* **2004**, *47*, 4463−4470.
(18) *Pipeline Pilot 2016*; Biovia: SanDiego, CA, USA, 2016, http://www.accelrys.com.
(19) Rogers, D.; Hahn, M. Extended-connectivity fingerprints. *J. Chem. Inf. Model.* **2010**, *50*, 742−754.
(20) A receiver operating characteristic (ROC) value indicates the accuracy of the model. The ROC value between 0.7 and 0.8 is considered as reasonable, 0.8−0.9 as good, and 0.9−1 as excellent.
(21) *Forge v.10.3;*Cresset: Litlington, UK, 2014, http://www.cresset-group.com.
(22) Cheeseright, T.; Mackey, M.; Rose, S.; Vinter, A. Molecular field technology applied to virtual screening and finding the bioactive conformation. *Expert Opin. Drug Discovery* **2007**, *2*, 131−144.
(23) Hawkins, P. C. D.; Skillman, A. G.; Warren, G. L.; Ellingson, B. A.; Stahl, M. T. Conformer generation with OMEGA: algorithm and validation using high quality structures from the protein databank and cambridge structural database. *J. Chem. Inf. Model.* **2010**, *50*, 572−584.
(24) *OMEGA 2.5;* OpenEye Scientific Software: Santa Fe, NM, 2020, http://www.eyesopen.com.
(25) Stienstra, R.; Duval, C.; Müller, M.; Kersten, S. PPARs, obesity, and inflammation. *PPAR Res.* **2007**, 1−10.
(26) The result of immunofluorescence analysis also revealed that compound **6** effectively inhibits PPAR-γ expression in 3T3-L1 cells. For details, see Figure S2.
(27) Berndt, J.; Kovacs, P.; Ruschke, K.; Klöting, N.; Fasshauer, M.; Schön, M. R.; Körner, A.; Stumvoll, M.; Blüher, M. Fatty acid synthase gene expression in human adipose tissue: association with obesity and type 2 diabetes. *Diabetologia* **2007**, *50*, 1472−1480.
(28) Berman, A. Y.; Motechin, R. A.; Wiesenfeld, M. Y.; Holz, M. K. The therapeutic potential of resveratrol: a review of clinical trials. *NPJ Precis. Oncol.* **2017**, *1*, 1−9.
(29) This compound can be purchased from Aurora Fine Chemicals (Austria).
(30) Tardugno, R.; Giancotti, G.; De Burghgraeve, T.; Delang, L.; Neyts, J.; Leyssen, P.; Brancale, A.; Bassetto, M. Design, synthesis and evaluation against Chikungunya virus of novel small-molecule antiviral agents. *Bioorg. Med. Chem.* **2018**, *26*, 869−874.
(31) *ROCS v.3.2.;* OpenEye Scientific Software: Santa Fe, NM, 2020, http://www.eyesopen.com.
(32) *EON v.2.2;* OpenEye Scientific Software: Santa Fe, NM, 2020, http://www.eyesopen.com.

https://dx.doi.org/10.1021/acsomega.9b04454
ACS Omega XXXX, XXX, XXX−XXX